Int. J. Appl. Comput. Math (2016) 2:699–711
DOI 10.1007/s40819-015-0105-z

ORIGINAL PAPER

Numerical Study of Effect of Inertia on Stability of Fibre Spinning

Renu Dhadwal[1]

Published online: 16 October 2015

Abstract Effect of inertia on the Draw resonance instability of Fibre spinning is studied numerically by carrying out a linear stability analysis of the governing equations. Viscoelastic effects are incorporated by using the Giesekus model as the constitutive equation. These results are validated by carrying out simulations of the complete non stationary system.

Keywords Fibre spinning · Giesekus model · Viscoelasticity · Draw resonance · Linear and nonlinear stability

Introduction

Fibre spinning is an important industrial process that has been studied widely in the past few years. There are different ways in which a fibre can be spun using molten polymer, for instance dry spinning, wet spinning and melt spinning. In this paper we particularly talk about melt spinning. In this process, molten polymer is extruded through a die also known as a spinn eret, subjected to cool air and then taken up via some take-up device at a velocity higher than the initial velocity. This ensures that the fibre is stretched. The ambient temperature is much lower than the polymer solidification point and therefore the polymer cools and solidifies before take-up. High speed non isothermal melt spinning is associated with a neck like deformation of the fibre, also known as "necking" where in there is a sudden and sharp decrease in the diameter of the fibre. The necking phenomena has been shown to be connected to flow induced crystallization in polymers [5]. Studies investigating this phenomena take into account the micro structure of the polymer molecules. In the industrial process hundreds of fibres are extruded and spun in parallel. But for our studies we consider only one fibre. Figure 1 shows a schematic diagram of the melt spinning process. The ratio of the take-up velocity (v_L) to the extrusion velocity (v_0) is called the Draw ratio ($D = \frac{v_L}{v_0} > 1$). Textile fibres need to conform

✉ Renu Dhadwal
renu.dhadwal@flame.edu.in

[1] Centre for Mathematical Modelling, FLAME University, Pune, India

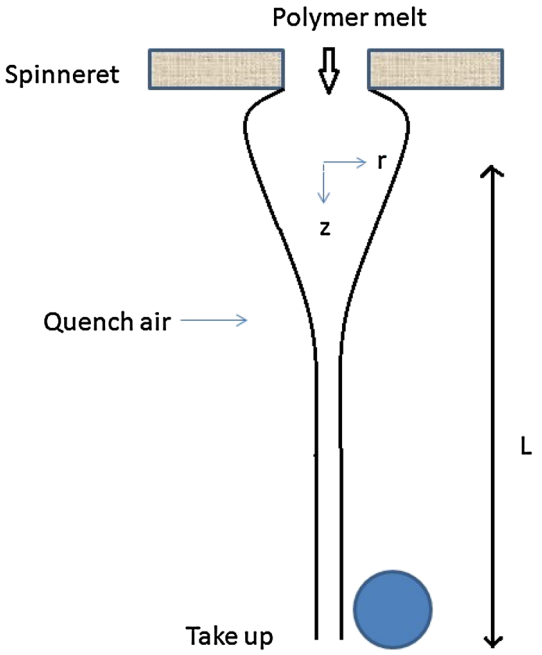

Fig. 1 Sketch of the melt spinning process

to prescribed dimensions and properties and therefore any fluctuations in the dimensions of the fibre need to be avoided. In order to prevent flow instabilities it is imperative to thoroughly understand not only the flow dynamics of the process but also the mechanical and rheological properties of the fluid. Among the different flow instabilities that can occur in a fibre spinning process the most severe is the filament breakup. This is connected to the necking phenomena [17]. The other important instability is called "Draw Resonance" and is characterized by sustained periodic oscillations in the cross-sectional area of the fibre. This happens when the Draw ratio exceeds a critical value. For Newtonian fluids this value has been numerically found to be of order 20, [3] and this has been corroborated through experimental results [4,9]. Since this instability makes it difficult to manufacture synthetic fibres at high speeds, it is worth studying the process of Draw resonance and factors that suppress it. Several factors such as inertia, spinline cooling and viscoelasticity are known to effect the stability of the spinning process. These have been investigated by several authors [10,12,14,15]. Spinline cooling has been shown to enhance stability where as surface tension tends to destabilise the spinning process. Stability of the spinning process has also been investigated by performing linear or spectral stability analysis [7,8,10,14]. It has long been established, [13,14] that inertia has a stabilising effect on spinning. This is easy to understand since conservation of mass requires that areas with large diameters move slowly and areas with smaller diameters move more rapidly. Effect of inertia is to inhibit the velocity which prevents changes in areas of the fibre. Hagen [6], has studied numerically the effect of inertia on the stability of the spinning process and given more precise and accurate results of the suppression of Draw resonance by inertia. However the study was limited to Newtonian fluids. Beris and Liu [1,2] in their seminal work have studied in detail the effect of inertia on Draw resonance dynamics using the Maxwell constitutive model. However, Maxwell model being a linear equation fails

to model the effects caused due to the nonlinear terms. Therefore, very often nonlinear models such as PTT and Giesekus are used in modeling processes involving viscoelastic flows.

In this work we investigate the fibre spinning equations using the Giesekus model. The Giesekus model describes how the relaxation time of a molecule is altered when the surrounding molecules are oriented. The relaxation behavior becomes anisotropic and results in an additional quadratic term of the stress tensor compared to the Maxwell model. The Giesekus model parameter α determines the magnitude of the anisotropic drag. In this work, effects such as necking are neglected as in order to incorporate those effects micro structure of the polymers would have to be taken into account. We are more interested in doing a qualitative analysis of a simple model governing the extensional flow of a polymer fluid with prescribed boundary conditions. First we derive analytic solutions of the stationary equations taking into account inertia as the dominant force but neglecting secondary forces such as gravity, surface tension and air drag. We then linearise the equations and perform a linear stability analysis. This is followed by the simulation of the complete nonlinear system of equations.

Description of the System

A polymer fibre is usually modeled as a uniaxial, extensional flow of fluid. Simple models consider the fluid to be Newtonian or simply viscous. But molten polymers are best described as viscoelastic fluids. Therefore, a viscoelastic model is used as the constitutive equation relating the stress to the strain rate. Considering the geometry of the fibre, usually a cylindrical coordinate system is used to describe the flow with the z coordinate in the direction of the flow. When the polymer melt exits the spinneret, it swells to several times its diameter size exhibiting a characteristic behavior of Non-Newtonian fluids also known as the "die swell effect". This phenomena has been ignored for simplicity. Since the radius of the fibre is very small in comparison to the length of the fibre, it is a common practice to consider one-dimensional (1-d) model equations. Considering the conservation laws of mass and momentum of a polymer jet and averaging over the cross-section of the fibre, the following one-dimensional equations are got [11].

$$\frac{\partial a}{\partial t} + \frac{\partial}{\partial z}(a v_z) = 0 \tag{1}$$

$$\rho a \left(\frac{\partial v_z}{\partial t} + v_z \frac{\partial v_z}{\partial z} \right) = \frac{\partial}{\partial z}(a \tau_{zz}) \tag{2}$$

In the above equations, z denotes the coordinate along the spinline, t is the time, a the cross sectional area of the fibre, v_z the axial velocity and τ_{zz} the axial stress. Radial stress variable is not considered. The energy equation has been neglected in order to get the isothermal process.

The constitutive equation of the Giesekus fluid has the form [16]

$$\boldsymbol{\tau} + \lambda \left(\frac{D\boldsymbol{\tau}}{Dt} - \mathbf{D}.\boldsymbol{\tau} - \boldsymbol{\tau}.\mathbf{D}^T \right) + \frac{\alpha \eta_0}{G} \boldsymbol{\tau}^2 = 2\eta_0 \dot{\epsilon} \tag{3}$$

where $\boldsymbol{\tau}$ denotes the stress tensor, $\mathbf{D}$ represents the deformation rate tensor, λ is the relaxation time of the polymer (time taken for the fluid to get back its original state after being stretched), η_0 is the zero-shear viscosity, G is the melt shear modulus and $\dot{\epsilon} = \frac{\mathbf{D}+\mathbf{D}^T}{2}$ denotes the rate-of-strain or extensional rate tensor. The Giesekus model parameter α is such that $0 \leq \alpha \leq 1$. For $\alpha = 0$, the isotropic, Upper Convected Maxwell model is recovered. The most severe case

of anisotropic drag is reached when $\alpha = 1$. In the above equation $\frac{D}{Dt}$ denotes the material derivative.

$$\frac{D}{Dt} = \frac{\partial}{\partial t} + \mathbf{v}.\Delta$$

where $\mathbf{v}$ is a velocity vector. Considering only the axial stress variable τ_{zz}, and integrating over the cross-sectional area, we get the following form of the Giesekus constitutive equation.

$$\tau_{zz} + \lambda\left(\frac{\partial \tau_{zz}}{\partial t} + v_z\frac{\partial \tau_{zz}}{\partial z} - 2\tau_{zz}\frac{\partial v_z}{\partial z}\right) + \frac{\alpha\eta_0}{G}\tau_{zz}^2 = 2\eta_0\frac{\partial v_z}{\partial z} \tag{4}$$

The system (1), (2) and (4) is subject to the following boundary conditions.
$a = a_0, \quad v_z = v_0, \quad$ at $z = 0$ for all t
$v_z = v_L \quad$ at $z = L$ for all t
where L denotes the length of the fibre, a_0 and v_0 denote the cross sectional area and axial velocity of the fibre at the spinneret and v_L denotes the take-up velocity of the fibre.

Dimensionless Equations

We non dimensionalise the equations by introducing the following dimensionless variables:

$$\tilde{a} = \frac{a}{a_0}, \quad \tilde{v} = \frac{v_z}{v_0}, \quad \tilde{t} = \frac{tv_0}{L}, \quad \tilde{z} = \frac{z}{L} \quad \tilde{\tau} = \frac{\tau_{zz}L}{\eta_0 v_0} \quad Re = \frac{\rho v_0 L}{\eta_0}, \quad De = \frac{\lambda v_0}{L}$$

The dimensionless transport equations governing the melt spinning process along with the constitutive equation are given below.

$$\frac{\partial \tilde{a}}{\partial \tilde{t}} + \frac{\partial(\tilde{a}\tilde{v})}{\partial \tilde{z}} = 0 \tag{5}$$

$$Re\,\tilde{a}\frac{\partial \tilde{v}}{\partial \tilde{t}} + Re\,\tilde{a}\tilde{v}\frac{\partial \tilde{v}}{d\tilde{z}} = \frac{\partial(\tilde{a}\tilde{\tau})}{\partial \tilde{z}} \tag{6}$$

$$\frac{\partial \tilde{\tau}}{\partial \tilde{t}} + \tilde{v}\frac{\partial \tilde{\tau}}{\partial \tilde{z}} - 2(\tilde{\tau} + \frac{1}{De})\frac{\partial \tilde{v}}{\partial \tilde{z}} = -\frac{\tilde{\tau}}{De}(1 + \alpha De\tilde{\tau}) \tag{7}$$

$$\tilde{z} = 0; \quad \tilde{a} = 1 = \tilde{v}, \tag{8}$$

$$\tilde{z} = 1; \quad \tilde{v} = D > 1 \tag{9}$$

In the above, De represents the dimensionless characteristic relaxation time, also known as the Deborah number and Re is the Reynolds number representing the force due to inertia, ρ being the density of the fiber. For sake of convenience hereafter we drop the ˜ from all the variables.

Steady State Solution

The stationary equations can be easily read off from Eqs. (5)–(7) as follows.

$$\frac{d(av)}{dz} = 0 \tag{10}$$

$$Re\,av\frac{dv}{dz} = \frac{d(a\tau)}{dz} \tag{11}$$

$$v\frac{d\tau}{dz} - 2\left(\tau + \frac{1}{De}\right)\frac{dv}{dz} = -\frac{\tau}{\mathrm{De}}(1 + \alpha De\tau) \tag{12}$$

From (10) and (11) we easily get $\tau = Rev^2 + cv$ where c is a constant. Substituting this in Eq. (12), we get the following differential equation in variable $v(z)$.

$$\frac{dv}{dz} = \frac{(cv + Rev^2)(1 + \alpha De(Rev^2 + cv))}{cvDe + 2}$$

Solving the above differential equation we get

$$\sqrt{\alpha De}(c^2De - 4Re)\tan^{-1}\frac{\sqrt{\alpha De}(c + 2Rev)}{\sqrt{4Re - \alpha c^2 De}} - \frac{cDe\log(\alpha vDe(c + Rev) + 1)}{2Re} + \frac{(c^2De - 2Re)\log(c + Rev)}{cRe} + \frac{2}{c}\log v = z + K \tag{13}$$

The constants K and c are got by applying the boundary conditions $v(0) = 1$ and $v(1) = D$ respectively. Let us have a look at some simplified cases.
Putting $\alpha = 0$ we get the solution with the UCM model,

$$\frac{(c^2De - 2Re)\log(c + Rev)}{cRe} + \frac{2}{c}\log v = z + K$$

Applying the boundary condition $v(0) = 1$ the following solution is got

$$\frac{2}{c}\log v(z) + \left(\frac{cDe}{Re} - \frac{2}{c}\right)\log\frac{Rev(z) + c}{Re + c} = z \tag{14}$$

This is the solution for the Maxwell fluid as got by [1]. Further by putting $Re = 0$ one gets the solution without the inertia terms

$$Dev(z) + \frac{2}{c}\log v(z) = z + De$$

where $c = \frac{2\log D}{1 + De - DeD}$

The solutions got above are implicit. In the following theorem we prove the existence of solution to the boundary value problem for the simple case of $\alpha = 0$.

Theorem 1 *Under the assumption that* $De > 0, 0 < Re < 4De\log(1 + 1/De)$, $e^{\sqrt{\frac{Re}{2De}}} < D < 1 + 1/De$, *there exists a number* $\tau_0 > Re + \sqrt{\frac{2Re}{De}}$ *such that there exists at least one solution of Eqs.* (10)–(12) *along with boundary conditions* (8) *and* (9)

Proof Consider the implicit solution as given by Eq. (14). Here, $c = \tau_0(D) - Re$ where τ_0 is an initial value of τ which depends on the Draw ratio D. Let

$$f(v) = \left(\frac{2}{\tau_0(D) - Re}\right)\log v(z) + \left(\frac{De(\tau_0 - Re)}{Re} - \frac{2}{\tau_0(D) - Re}\right)\log\left(\frac{Rev(z) + \tau_0(D) - Re}{\tau_0(D)}\right) - z$$
$$\lim_{v\to 0} f(v) = -\infty \tag{15}$$

Also,

$$\lim_{v\to\infty} f(v) = \infty \tag{16}$$

Hence, from the intermediate value theorem, there exists at least one solution $v \in (0, \infty)$. Now substituting the boundary condition $v(1) = D$ in Eq. (14) we get

$$\left(\frac{(\tau_0 - Re)^2 De - 2Re}{(\tau_0 - Re)Re}\right) \log\left(\frac{\tau_0 - Re + ReD}{\tau_0}\right) + \frac{2}{(\tau_0 - Re)} \log D = 1$$

Let

$$g(\tau_0) = \left(\frac{(\tau_0 - Re)^2 De - 2Re}{(\tau_0 - Re)Re}\right) \log\left(\frac{\tau_0 - Re + ReD}{\tau_0}\right) + \frac{2}{(\tau_0 - Re)} \log D - 1$$

$$\lim_{\tau_0 \to Re + \sqrt{\frac{2Re}{De}}} g(\tau_0) = \sqrt{\frac{2De}{Re}} \log D - 1 > 0 \quad \text{since } D > e^{\sqrt{\frac{Re}{2De}}}$$

Also,

$$\lim_{\tau_0 \to \infty} g(\tau_0) = De(D-1) - 1 < 0 \quad \text{since } D < 1 + 1/De$$

Therefore, using the intermediate value theorem, there exists at least one $\tau_0 \in (Re + \sqrt{\frac{2Re}{De}}, \infty)$ such that the boundary value problem has a solution. □

The proof of existence of stationary solutions for $\alpha \neq 0$ may be investigated using fixed point arguments which may be the subject of another paper.

Numerical Method

Numerical method for solving the stationary boundary value problem consists of the following steps:

1 Initialise i = 2
2 Guess two boundary conditions for stress at $z = 0$, namely s^1 and s^2. Let s^i denote the value of $\tau(0)$ in the ith iteration.
3 Solve the system of odes twice as an initial value problem with two initial condition vectors $(a(0), v(0), s^{i-1})$ and $(a(0), v(0), s^i)$.
4 Compute the error $\epsilon = |D - v(s^i, 1)|$.
5 Let Tol denote a prescribed tolerance. If $\epsilon > Tol$ then,

- compute the new value of $\tau(0)$ using the secant method as follows:

$$s^{i+1} = s^{i-1} + (s^i - s^{i-1}) \frac{D - v(s^i, 1)}{v(s^i, 1) - v(s^{i-1}, 1)}$$

- update $i = i + 1$
- go to step 3 and follow the procedure only for the latest value of i.

else
Stop

Figure 2 shows the typical axial velocity profiles of a fibre for various values of α in the stationary case. The axial velocity increases to match the axial velocity prescribed at the end.

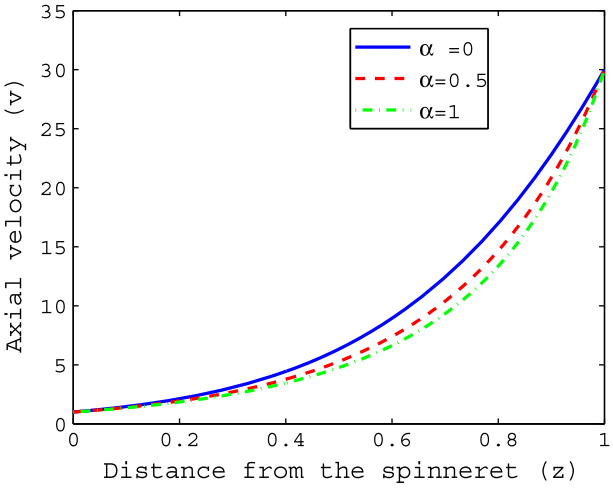

Fig. 2 Axial velocity profiles of the stationary solutions for $De = 0.005$, $Re = 0.01$, $D = 30$ for various values of α

Linear Stability Analysis

Equipped with the existence of stationary solutions, we proceed to linearise the equations and perform a linear stability analysis. We introduce infinitesimal perturbations in the steady state solutions as follows.

$$a(t,z) = a_s(z) + \gamma(z)\exp(\mu t),\ \ v(t,z) = v_s(z) + \beta(z)\exp(\mu t),$$
$$\tau(t,z) = \tau_s(z) + \phi(z)\exp(\mu t)$$

where a_s, v_s and τ_s are the steady state solutions. Substituting these in Eqs. (5)–(9) and neglecting higher order terms we get the following system.

$$\begin{aligned}
\mu\gamma &= -v_s'\gamma - v_s\gamma' - a_s'\beta - a_s\beta' \\
\mu\beta &= \gamma\left(\frac{\tau_s{}'}{Rea_s} - \frac{v_s v_s'}{a_s}\right) + \gamma'\left(\frac{\tau_s}{Rea_s}\right) - \beta v_s' - \frac{\beta'}{a_s} + \phi\left(\frac{a_s'}{Rea_s}\right) + \frac{\phi'}{Re} \\
\mu\phi &= -\tau_s{}'\beta + \beta' 2\left(\tau_s + \frac{1}{De}\right) + \phi\left(2v_s' - \alpha\tau_s - \frac{1+\alpha De\tau_s}{De}\right) - v_s\phi'
\end{aligned} \tag{17}$$

where $\gamma' = \frac{d\gamma}{dz}$.
Boundary conditions: $\gamma(0) = \beta(0) = \beta(1) = 0$.
There are several discretization schemes that can be used to solve the above system of equations. In the context of fibre spinning equations, Chebyschev collocation scheme has proven to be robust [6]. Therefore, we employ this method to find the eigenvalues of the above system. The unknowns γ, β and ϕ are projected onto the vector space of functions spanned by the Chebyshev polynomials $\{\mathcal{C}_n\}_0^N$ of degree 0 through N.

$$\gamma^N(z) = \sum_{n=0}^{N}\gamma_n\mathcal{C}_n(2z-1),\ \beta^N(z) = \sum_{n=0}^{N}\beta_n\mathcal{C}_n(2z-1),\ \phi^N = \sum_{n=0}^{N}\phi_n\mathcal{C}_n(2z-1)$$

with $3(N+1)$ unknown coefficients $\gamma_n, \beta_n, \phi_n$. These projections are substituted in the Eqs. (5)–(9) and evaluated at the $N+1$ collocation points $z_k = \frac{1}{2}\left(\cos\left(\frac{\pi k}{N}\right)+1\right), \quad 0 \le k \le N$. This gives the following discretised eigenvalue problem to be solved.

$$\mu B\mathbf{u} = A\mathbf{u} \tag{18}$$

where $\mathbf{u} = [\gamma_n, \beta_n, \phi_n]$. The eigenvalues are got by using the function "eig.m" in MATLAB. Eigenvalues are computed for increasing values of N until convergence is achieved. In our computations N = 600 was good enough to give us the required convergence.

Results of Linear Stability Analysis

Figure 3 is the stability diagram which shows the pairings of Draw ratio D and Deborah number De with $Re = 0$ for $\alpha = 0$. As mentioned before, $\alpha = 0$ reduces the Giesekus model to the UCM model for which a detailed stability analysis has been done by Beris

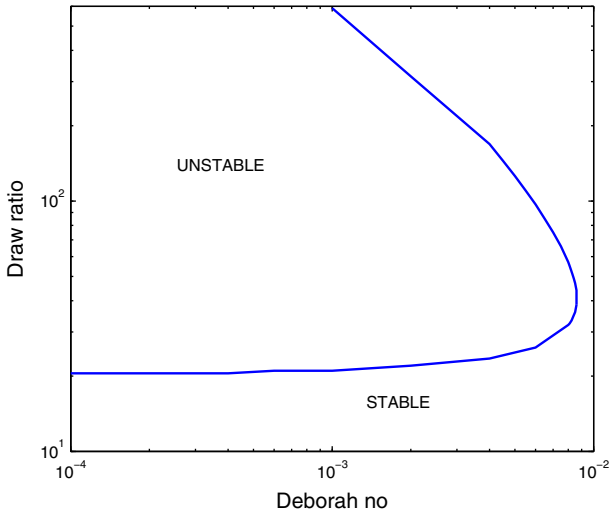

Fig. 3 Stability diagram for Deborah number versus Draw ratio for $\alpha = 0$, $Re = 0$

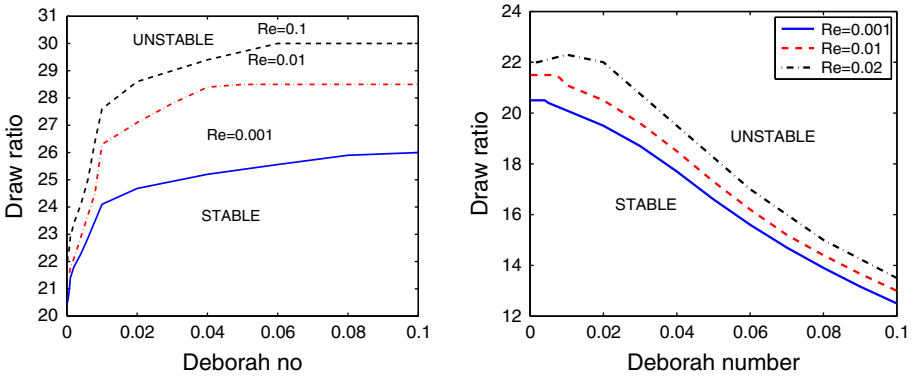

Fig. 4 Stability diagram for Re versus Draw ratio for $\alpha = 0.2$ (*left*), $\alpha = 0.5$ (*right*)

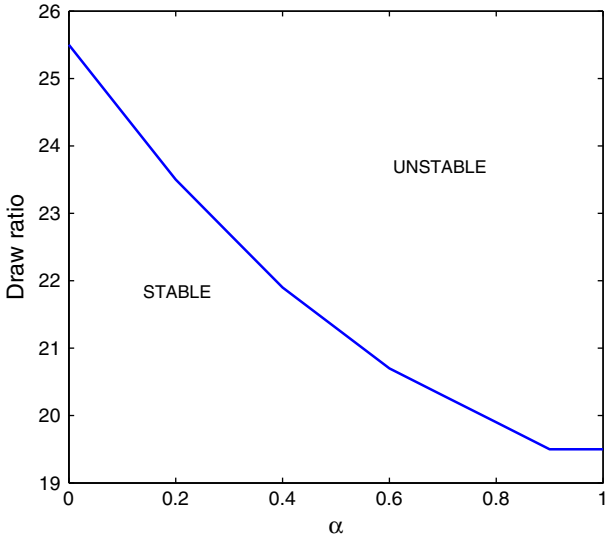

Fig. 5 Stability diagram for α versus Draw ratio for $De = 0.005$, $Re = 0.01$

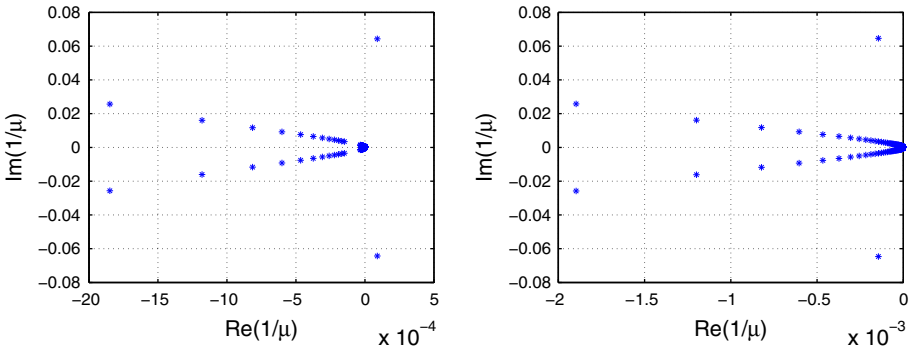

Fig. 6 Eigenspectra for $\alpha = 0$, $De = 0.005$, $D = 25$, $Re = 0.002$ (*left*), $Re = 0.008$ (*right*)

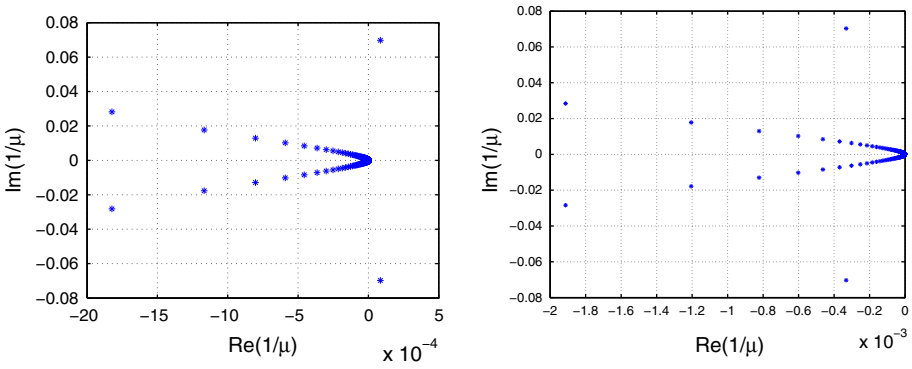

Fig. 7 Eigenspectra for $\alpha = 0.2$, $De = 0.002$, $D = 22.8$, $Re = 0.01$ (*left*), $Re = 0.02$ (*right*)

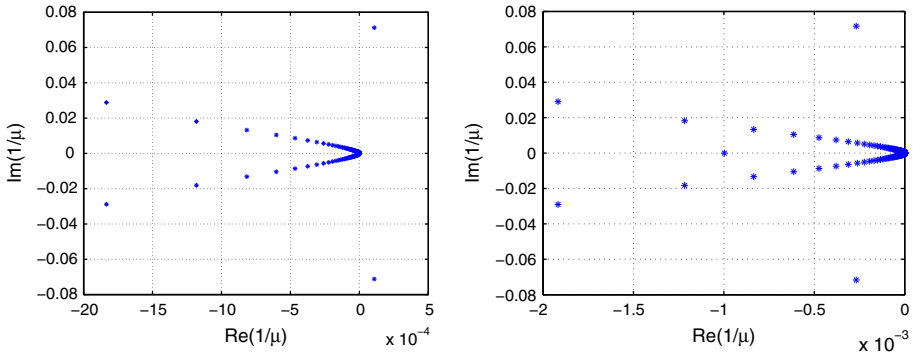

Fig. 8 Eigenspectra for $\alpha = 0.5$, $De = 0.001$, $D = 20.5$, $Re = 0.001$ (*left*), $Re = 0.01$ (*right*)

and Liu [1]. The given figure compares well with the stability diagram as produced by the mentioned authors, for low to medium range of Draw ratios. Since computations become more difficult with increasing Draw ratios and the purpose of this paper is to study the Draw resonance instability for various Giesekus fluids, we limited our computations to medium range of Draw ratios. The instability region that we get differs from that of the Newtonian fibre, considerably in that in the viscoelastic case it tends to be closed. Figure 4 shows us the stability regions for Giesekus fluids with $\alpha = 0.2$ and $\alpha = 0.5$ respectively. These figures vary considerably from the case where $\alpha = 0$. For $\alpha = 0.2$, the stability curve seems to plateau with increasing value of De. In the case where $\alpha = 0.5$, it is interesting to note as De increases stability decreases. Figure 5 shows that as the values of α increase, stability comes down. Increase in nonlinearity of stress in the Giesekus model, decreases stability. Effect of inertia however is to increase the stability in all cases although as α increases, the stability is only marginally improved.

Figures 6, 7 and 8 show us the spectra for various values of α for constant Draw ratio and a slightly varying Re keeping all other parameters fixed. We have plotted the inverse of eigenvalues so that the complete spectrum is visible.The eigenspectra are lined up along certain curves. As Re is increased slightly, the dominant pair of the complex-conjugate eigenvalue crosses over to the left half of the plane showing the transition from instability to stability. This is an indicator of the occurrence of a subcritical Hopf bifurcation.

Non Stationary Equations

The system of Eqs. (5–9) is solved numerically using the Method of Lines. We set $h = 1/N$ and $x_i = \frac{i}{N}$, where N is the number of nodes and $0 \leq i \leq N$. Define $a_i(t) = a(x_i, t)$, $v_i(t) = v(x_i, t)$ and $\tau_i(t) = \tau(x_i, t)$. An upwind method is used to approximate the convective derivatives. The other spatial derivatives are approximated using central differences at the interior nodes, $1 \leq j \leq N - 1$.

$$\frac{da_j}{dt} = -a_j \frac{(v_{j+1} - v_{j-1})}{2h} - v_j \frac{(a_j - a_{j-1})}{h} \tag{19}$$

$$\frac{dv_j}{dt} = -v_j \frac{(v_j - v_{j-1})}{h} + \frac{1}{Re} \frac{(\tau_{j+1} - \tau_{j-1})}{2h} + \frac{\tau_j}{Rea_j} \frac{(a_{j+1} - a_{j-1})}{2h} \tag{20}$$

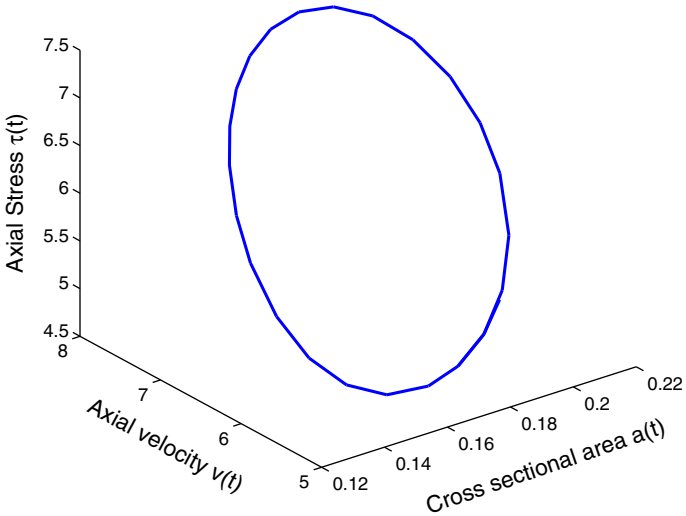

Fig. 9 Limit cycle $\alpha = 0$, $D = 26$, $De = 0.005$, $Re = 0.002$ at $z = 1/2$

$$\frac{d\tau_j}{dt} = -v_j \frac{(\tau_j - \tau_{j-1})}{h} + 2\left(\tau_j + \frac{1}{De}\right)\frac{(v_{j+1} - v_{j-1})}{2h} - \frac{\tau_j}{De}(1 + \alpha De \tau_j) \quad (21)$$

Stress boundary condition at $z = 0$ is not specified. Therefore the spatial derivatives in the stress equation at the first node are discretized using forward differences and the resulting equation reads as follows.

$$\frac{d\tau_0}{dt} = -\frac{(\tau_1 - \tau_0)}{h} + 2\left(\tau_0 + \frac{1}{De}\right)\frac{(v_1 - 1)}{h} - \frac{\tau_0}{De}(1 + \alpha De \tau_0) \quad (22)$$

The area and stress evolution equations at $j = N$ are got by discretizing the spatial variables using backward differences.

$$\frac{da_N}{dt} = -a_j \frac{(D - v_{N-1})}{h} - D\frac{(a_N - a_{N-1})}{h} \quad (23)$$

$$\frac{d\tau_N}{dt} = -D\frac{(\tau_N - \tau_{N-1})}{h} + 2\left(\tau_N + \frac{1}{De}\right)\frac{(D - v_{N-1})}{h} - \frac{\tau_N}{De}(1 + \alpha De \tau_N) \quad (24)$$

Boundary conditions: $a_0(t) = 1$, $v_0(t) = 1$ and $v_N(t) = D(1 + \delta)$ where $\delta > 0$ represents the perturbation in the actual Draw ratio.
Initial conditions: $a_i(0) = a_s$, $v_i(0) = v_s$ and $\tau_i(0) = \tau_s$ for $1\,0 \le i \le N$
where a_s, v_s and τ_s are the steady state solutions. Here, ϵ is the perturbation introduced in the Draw ratio. The resulting system is a first order system of ODEs in 3N unknowns which is solved using standard MATLAB ode solvers.

Results of Nonstationary Simulations

Figures 10, 11 and 12 show the graphs of cross sectional area versus time at $z = 1$ for the same set of parameters as in Figs. 6, 7 and 8 respectively. For instance, consistent with the linear stability results, we see that the Draw resonance instability manifests at $D = 26$

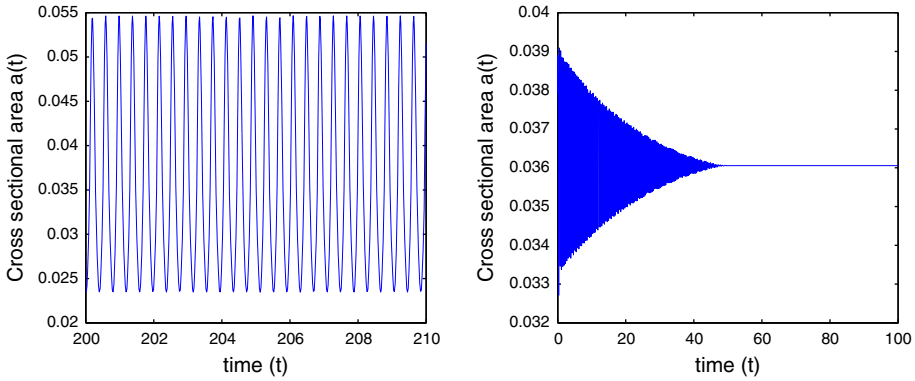

Fig. 10 Area versus time at $z = 1$ for $\alpha = 0$, $Re = 0.002$, $De = 0.005$, $D = 26$ (*left*), $Re = 0.008$ (*right*)

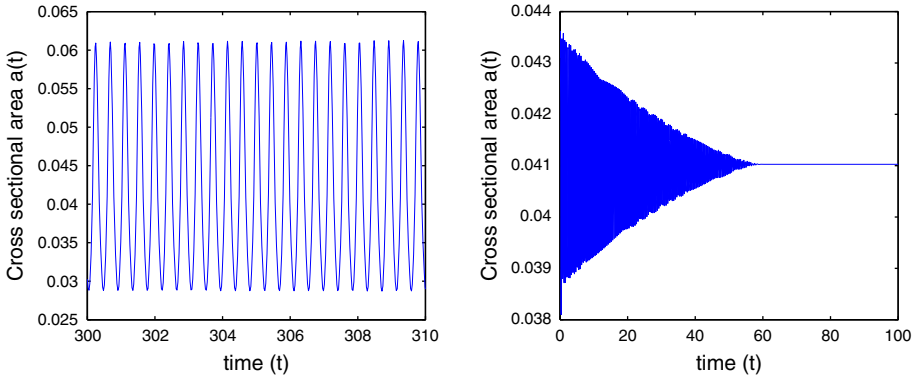

Fig. 11 Area versus time at $z = 1$ for $\alpha = 0.2$, $Re = 0.01$, $De = 0.005$, $D = 23$ (*left*), $Re = 0.02$ (*right*)

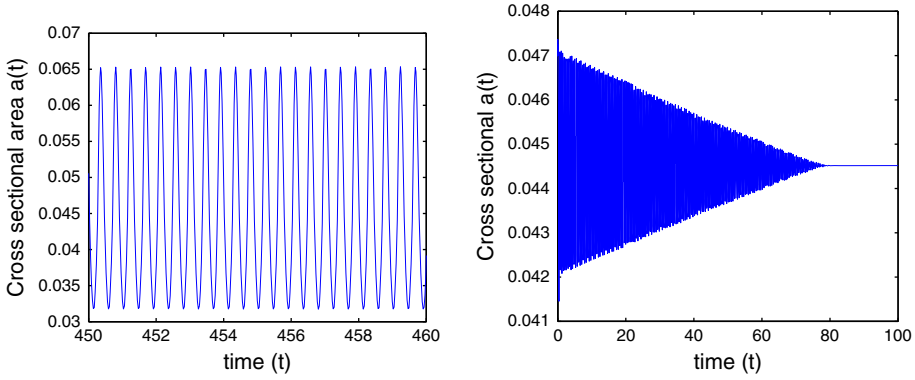

Fig. 12 Area versus time at $z = 1$ for $\alpha = 0.5$, $Re = 0.001$, $De = 0.001$, $D = 21$ (*left*), $Re = 0.01$ (*right*)

and $Re = 0.002$ for $\alpha = 0$ in the form of sustained periodic oscillations in the cross-sectional area of the fibre. Also, as the value of Re is increased slightly keeping the draw ratio constant, the oscillations in the cross sectional area of the fibre dampen to finally reach the steady state solution. It is a well known fact that in the terminology of nonlinear dynamics

Draw resonance presents itself as a Hopf bifurcation. When the complex conjugate pair of eigenvalues crosses the imaginary axis from right half plane to the left half as the values of the parameter Re is increased, it is the case of occurrence of a subcritical Hopf bifurcation. This has been demonstrated in the plots of the eigenspectra. The instability presents itself in the form of time periodic sustained oscillations. Figure 9 shows a section of the Limit cycle corresponding to a time periodic motion.

Conclusion

In conclusion, in this paper we have furnished a numerical study of the suppression of Draw resonance due to inertia in the fibre spinning process by doing a linear stability analysis as well as by simulating the nonstationary equations using a nonlinear viscoelastic constitutive equation. Along with the plots of complete eigenspectra and corresponding nonstationary simulations, we furnish stability diagrams showing the stability regions for various values of the Giesekus parameter α which describe Giesekus fluids with varying anisotropic drag. We believe that since this work is new, it certainly adds to our knowledge about the role of inertia in suppressing Draw resonance in nonlinear viscoelastic fibres.

References

1. Beris, A.N., Liu, B.: Time-dependent fiber spinning equations. 1. Analysis of the mathematical behaviour. J. Non-Newton. Fluid Mech. **26**, 341–361 (1988)
2. Beris, A.N., Liu, B.: Time-dependent fiber spinning equations. 1. Analysis of the stability of numerical approximations. J. Non-Newton. Fluid Mech. **26**, 363–394 (1988)
3. Cao, J.: Numerical simulations of draw resonance in melt spinning of polymer fluids. J. Appl. Polym. Sci. **49**, 1759 (1993)
4. Demay, Y., Agassant, J.F.: Experimental study of the draw resonance in fiberspinning. J. Non-Newton. Fluid Mech. **18**, 187 (1985)
5. Doufas, A.K., McHugh, A.J., Miller, C.: Simulation of melt spinning including flow induced crystallization. Part1 model development and prediction. J. Non-Newton. Fluid Mech. **92**, 27–66 (2000)
6. Hagen, T., Langwallner, B.: A numerical study on the suppression of draw resonance by inertia. Z. Angew. Math. Mech **86**(1), 63–70 (2006)
7. Hyun, J.: Theory of draw resonance: I. Newtonian fluids. AIChE J. **24**, 418 (1978)
8. Hyun, J.: Theory of draw resonance: Part II. Power-law and maxwell fluids. AIChE J. **24**, 423 (1978)
9. Kase, S.: Studies on melt spinning. IV. Stability of melt spinning. J. Appl. Polym. Sci. **18**, 3279 (1974)
10. Kase, S., Matsuo, T.: Studies on melt spinning. I. Fundamental equations on the dynamics of melt spinnning. J. Polym. Sci. Part A **3**, 2541–2554 (1965)
11. Langtangen, H.P.: Derivation of a Mathematical Model for Fibre Spinning. Department of Mathematics, Mechanics Division, University of Oslo, Oslo (1997)
12. Lee, J., Jung, H., Kim, S., Hyun, J.: Effect of fluid viscoelasticity on draw resonance dynamics of melt spinning. J. Non-Newton. Fluid Mech. **99**, 159–166 (2001)
13. Pearson, J.R.A.: Mechanics of Polymer Processing. Springer (1985)
14. Pearson, J.R.A., Shah, Y.T.: On the stability of isothermal and non-isothermal fibre spinning of powerlaw fluids. Ind. Eng. Fundam. Chem. **13**(2), 134–138 (1974)
15. Shin, D.M., Lee, J.S., Jung, H.W., Hyun, J.C.: Analysis of the effect of flow-induced crystallization on the stability of low-speed spinning using linear stability method. Korea-Aust. Rheol. J. **17**(2), 63–69 (2005)
16. Tanner, R.I.: Engineering Rheology. Oxford Science Publications, Oxford (1988)
17. Ziabicki, A.: Fundamentals of Fiber Formation. Wiley, New York (1976)